ELSEVIER
International Journal of Solids and Structures 41 (2004) 5425–5446
INTERNATIONAL JOURNAL OF SOLIDS and STRUCTURES
www.elsevier.com/locate/ijsolstr

Thickness flexible sandwich theory for the common description of global and local effects

Arnold Kühhorn *, Mark Golze

Chair of Structural Mechanics and Vibration of Vehicles, Brandenburg University of Technology, Siemens-Halske-Ring 14, 03044 Cottbus, Germany

Received 7 June 2002; received in revised form 9 March 2004
Available online 8 May 2004

Abstract

An advanced design of sandwich structures requires not only knowledge of global stress- and deformation behaviour, but also knowledge of local effects, such as load singularities and loss of stability caused by short wave wrinkling of one (bending load) or both (compressive load) sandwich skins.

Based on the nonlinear theory for sandwich shells with seven kinematic degrees of freedom, introduced by Kühhorn (1991, 1993) and Kühhorn and Schoop (1992), an improved theory for plane sandwich shells with eight degrees of freedom is presented, taking into account the core warping, which enables a much better representation of the sandwich core behaviour. Because of consideration of quadratic core thickness, linear core shear strain, and longitudinal core deformation, prediction of wrinkling behaviour can be improved even for moderately thick cores with comparably thin skins. The kinematic quantities as well as the nonlinear differential equations and the simplified equations of first-order theory resulting from them are presented. Short numerical examples demonstrate the efficiency of the theory.

Keywords: Sandwich; Thickness flexible; Wrinkling; Instability; Plate theory

1. Introduction

Sandwich (SW) structures are three-layer high performance lightweight structures (Wiedemann, 1986; Plantema, 1966; Stamm and Witte, 1974, among others) consisting of a soft core which is covered by stiff skin layers (Fig. 1). They are characterised by both excellent bending stiffness and low weight. However, due to their comparatively high shear flexibility, the global behaviour concerning deflection and buckling is described by a shear flexible theory of the Reissner (1945)/Mindlin (1951)-type where only the membrane stresses in the thin skin layers are considered, whereas the in-plane stresses appearing in the core are

* Corresponding author. Tel.: +49-355-69-4817; fax: +49-355-69-4805.
E-mail addresses: arnold.kuehhorn@tu-cottbus.de (A. Kühhorn), golze@tu-cottbus.de (M. Golze).

0020-7683/$ - see front matter
doi:10.1016/j.ijsolstr.2004.04.004

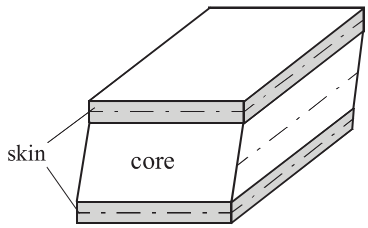

Fig. 1. Sandwich construction.

neglected. This theory is known as the Sandwich Membrane Theory (SWMT, see Wiedemann, 1986; Plantema, 1966, among others) which has proven to be reliable for a long time.

Indeed SW-structures under compressive loads show, besides global instability cases (buckling), also local instability phenomena such as short wave wrinkling of one or both skin layers (Fig. 2). Aiming at a determination of the failure-relevant wrinkling membrane stresses in the skin caused by compressive loads, separate formulas (Stamm and Witte, 1974; Vonach and Rammerstorfer, 2000, among others) have been developed for estimation purposes; they take into account skin and core parameters. Furthermore, the behaviour of SW-structures depends on load application because which often disturbs the state of membrane stresses in the skins.

For an at least approximate description of both global structural behaviour of SW and local phenomena, the SWMT must be extended. For this purpose Kühhorn (1991, 1993) and Kühhorn and Schoop (1992) presented a thickness flexible, geometrically nonlinear SW-shell theory using seven kinematic degrees of freedom. This theory is able to solve the problems mentioned above with sufficient accuracy if the local pertubations considered are characterised by wavelengths which are not too short (numerical investigations show that this theory is applicable for wrinkling problems characterised by half waves longer than 0.8-times of the core thickness). This extended theory includes the independent bending stiffness of each skin separately. Also a linear thickness stretch distribution over the height of the core is taken into account whereas the core in-plane stresses remain unconsidered.

In order to accurately describe even pertubations characterised by shorter wavelengths, the theory mentioned above will be extended. Therefore a geometrically nonlinear thickness flexible theory for plane SW-structures using eight kinematic degrees of freedom, with special emphasis on core warping, will be presented. The generalised SW-core description is based on a compatible (at least in first-order theory) core displacement field that approximates the three-dimensional strain and stress state sufficiently and also takes core warping into account. Inside the SW-core this extension results in a quadratic description of the thickness stretch over the height and a linear transversal shear strain as well as an in-plane strain up to the

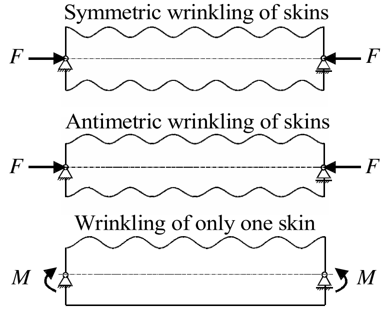

Fig. 2. Local instability cases.

fourth order. In this way the wrinkling problem and the stresses (peeling- and shear stresses) in the contact zone between the core and the covering skins, essential for failure of a SW-structure, are indicated more accurately.

Frequently, the study of local behaviour of SW-structures is done considering thick skin layers with a thin core and thin skin layers with a thick core (see Section 3). Generally, with this nomeclature, the long- and short-wave decay behaviour of disturbances shall be characterised. Because of the dependency on geometrical relation (skin/core thickness $\approx t/h$) and the different material stiffnesses (skin/core $\approx {}^{s}E/{}^{c}E$), a relation between wrinkling half-wavelength a and core thickness h (a/h or a/d, with $d = h + t$) would be a more exact identification.

The design of the following two-dimensional SW-theory is closely related to the works of Naghdi (1972) and others (Simo et al., 1990; Frostig, 1998; Krätzig, 1993; Schoop, 1988; Bischoff and Ramm, 2000; Vonach and Rammerstorfer, 2001, among others), which deal with extended shell/plate kinematics. The aim of this work is an enhanced kinematic description specialised for classical three layered and symmetric SW-structures using as few degrees of freedom as is sufficient to represent not only the global but also, at least approximately, the local behaviour such as, e.g., short wave wrinkling.

At first, in order to achieve greater clarity, the derivations of kinematic and static quantities will be presented separately for skin and core.

2. Geometrically nonlinear, thickness flexible theory with generalised core warping for plane sandwich structures

2.1. Requirements and assumptions

SW-structures are considered to be plane and two-dimensional with the following properties:

- They are three-layered and symmetric in respect to the midplane.
- The core material is substantially softer than the skin material (${}^{c}E \ll {}^{s}E$); both materials are considered to be homogeneous (in case of inhomogeneous materials (e.g. core made of Honeycomb) homogenised data has to be used).
- In the undeformed reference configuration the thicknesses of core and skins should be constant.
- For the SW-skins the Kirchoff/Love theory is valid; that means flexible in stretching and bending but rigid against shear.

2.2. Kinematic and static quantities of the SW-skins

The development of the required kinematic description is based on the fact that the membrane strains of the skins and the shear strain of the core are relevant for representation of the global behaviour (SWMT, 5 DOF). The description of local effects requires, in addition, consideration of the individual skin curvatures and, because the core must support both skins, consideration of its transversal and in-plane deformations is necessary (three additional DOFs) as well.

The following kinematic modelling of the SW is based on parameters which are defined with regard to the midsurface. In detail these parameters are the position vector $\boldsymbol{r}$ and the director $\boldsymbol{d}$ as well as two intensity coefficients α_{z1} and α_{z2}, mainly interpreted as the linear and quadratic parts of the core thickness strain, both of which are linked with the associated core cross-section warpings.

The following geometric SW-parameters are introduced: t: thickness of SW-skin, h: thickness of SW-core, $d = h + t$: distance between skin midsurfaces.

Further, quantities are denoted with a top right index, where ψ^i, $i = 1, 2$: refers to the skins in general, whereas the upper skin is denoted by $i = 1$ and the lower skin by $i = 2$.

In the case of a missing top right index, ψ is defined with regard to the geometric midsurface.

Using Lagrangian coordinates q^α of the midsurface for the description of a material point in the undeformed configuration by $\boldsymbol{X}^i(q^\alpha)$ and in the deformed configuration by $\boldsymbol{x}^i(q^\alpha)$, the vectors of the geometric midsurface (Fig. 3) are defined as follows:

$$\boldsymbol{R}(q^\alpha) = \frac{1}{2}(\boldsymbol{X}^1 + \boldsymbol{X}^2) \quad \text{and} \quad \boldsymbol{r}(q^\alpha) = \frac{1}{2}(\boldsymbol{x}^1 + \boldsymbol{x}^2), \tag{1}$$

$$\boldsymbol{n}(q^\alpha) = \frac{1}{d}(\boldsymbol{X}^1 - \boldsymbol{X}^2), |\boldsymbol{n}| = 1 \quad \text{and} \quad \boldsymbol{d}(q^\alpha) = \frac{1}{d}(\boldsymbol{x}^1 - \boldsymbol{x}^2), |\boldsymbol{d}| \neq 1. \tag{2}$$

The material points of the two skin midsurfaces (see Eqs. (1) and (2)) are defined in a way that in case of identical midsurface coordinates q^α the vector connecting these two points in the reference configuration ($d\boldsymbol{n}$) is perpendicular to the midsurface (Fig. 3).

For reasons of simpler comparison with other works (Kühhorn, 1991, 1993; Kühhorn and Schoop, 1992; Schoop, 1988; Schoop, 1999), the definition of the director $\boldsymbol{d}$ remains unmodified, but it can also be expressed by the vectors $\boldsymbol{n}$ and $\boldsymbol{w}$ as in the following equation:

$$\boldsymbol{d} = \frac{\overline{\boldsymbol{a}}_3}{d/2} = \boldsymbol{n} + \frac{\boldsymbol{w}}{d/2}, \quad \text{where } \boldsymbol{w} = \frac{d}{2}(\boldsymbol{d} - \boldsymbol{n}). \tag{3}$$

See for example the papers of Bischoff and Ramm (2000) or Büchter et al. (1994).

2.2.1. Kinematics of the SW-skins

According to Fig. 3 and Eqs. (1) and (2) the exact description of the skin midsurfaces is given by the midsurface vectors as follows:

$$\boldsymbol{X}^i(q^\alpha) = \boldsymbol{R} \pm \frac{d}{2}\boldsymbol{n} \quad \text{and} \quad \boldsymbol{x}^i(q^\alpha) = \boldsymbol{r} \pm \frac{d}{2}\boldsymbol{d} \tag{4}$$

with the additional condition that the triple scalar product $[\boldsymbol{d}, \boldsymbol{r}_{,1}, \boldsymbol{r}_{,2}] > 0$ remains positive (no penetration). The Nabla-operator

$$\boldsymbol{\nabla} = \boldsymbol{\nabla}_2 + \boldsymbol{n}\frac{\partial}{\partial z} \quad \text{is divided into} \quad \boldsymbol{\nabla}_n = \boldsymbol{n}\frac{\partial}{\partial z} \quad \text{and} \quad \boldsymbol{\nabla}_2 = \boldsymbol{a}^\alpha \frac{\partial}{\partial q^\alpha}, \tag{5}$$

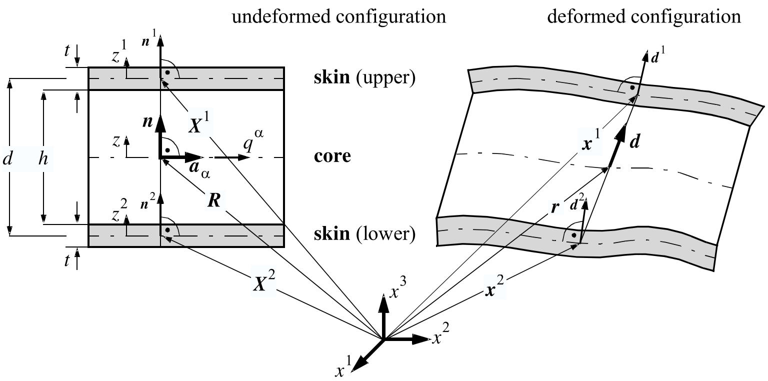

Fig. 3. Kinematic description of the SW-skins and the midsurface.

where ∇_n denotes the transversal and ∇_2 the in-plane part and where $\boldsymbol{a}^\alpha$ is the reciprocal base for $\boldsymbol{a}_\alpha = \partial\boldsymbol{R}/\partial q^\alpha = \boldsymbol{R}_{,\alpha}$ with respect to the generally curvilinear coordinates q^α. Therefore the following relation holds:

$$\nabla_2 \otimes \boldsymbol{R} = \boldsymbol{a}^\alpha \otimes \boldsymbol{R}_{,\alpha} = \boldsymbol{E}_2 \stackrel{\wedge}{=} \delta_{\alpha\cdot}^{\cdot\beta} \boldsymbol{a}^\alpha \otimes \boldsymbol{a}_\beta. \tag{6}$$

$\boldsymbol{E}_2$ represents the in-plane unit tensor and $\otimes$ stands for the dyadic or tensorial product, respectively. If Cartesian coordinates $q^\alpha = X^\alpha$ are used, the in-plane part of (5) is simplified to $\nabla_2 = \boldsymbol{e}_\alpha \partial/\partial X^\alpha$ and $\boldsymbol{a}^\alpha = \boldsymbol{a}_\alpha = \boldsymbol{e}_\alpha$, where $\boldsymbol{e}_\alpha$ is the orthonormal base. Further developments are based on the introduction of the gradient tensors of the midsurface vectors. These tensors are planar with respect to the undeformed and spatial with regard to the deformed configuration:

$$\boldsymbol{F} = \mathrm{Grad}^{\mathrm{T}}\boldsymbol{r} = (\nabla_2 \otimes \boldsymbol{r})^{\mathrm{T}} = (\boldsymbol{r}_{,\alpha} \otimes \boldsymbol{a}^\alpha)^{\mathrm{T}}, \tag{7}$$

$$\boldsymbol{G} = \mathrm{Grad}^{\mathrm{T}}\boldsymbol{d} = (\nabla_2 \otimes \boldsymbol{d})^{\mathrm{T}} = (\boldsymbol{d}_{,\alpha} \otimes \boldsymbol{a}^\alpha)^{\mathrm{T}}. \tag{8}$$

2.2.2. Membrane strain of the SW-skins

The application of (5) to (4) leads to

$$\boldsymbol{F}^i = (\nabla_2 \otimes \boldsymbol{x}^i)^{\mathrm{T}} = \left(\nabla_2 \otimes \left(\boldsymbol{r} \pm \frac{d}{2}\boldsymbol{d}\right)\right)^{\mathrm{T}} = \boldsymbol{F} \pm \frac{d}{2}\boldsymbol{G} \quad (i = 1, 2), \tag{9}$$

whereat the in-plane Green–Lagrangian membrane strain tensor of skin i is defined as

$$\boldsymbol{D}^i = \frac{1}{2}(\boldsymbol{F}^{i\mathrm{T}} \cdot \boldsymbol{F}^i - \boldsymbol{E}_2) = \frac{1}{2}\left\{\left(\boldsymbol{F}^{\mathrm{T}} \cdot \boldsymbol{F} - \boldsymbol{E}_2 + \frac{d^2}{4}\boldsymbol{G}^{\mathrm{T}} \cdot \boldsymbol{G}\right) \pm \frac{d}{2}(\boldsymbol{F}^{\mathrm{T}} \cdot \boldsymbol{G} + \boldsymbol{G}^{\mathrm{T}} \cdot \boldsymbol{F})\right\}. \tag{10}$$

2.2.3. Curvature of the SW-skins

The complexities within the invariant description of the individual skin bending strains due to the consideration of the Kirchhoff-Hypothesis require an indirect procedure. Using the auxiliary directors $\boldsymbol{d}^i$ (Fig. 3) of the skins, and assuming that these remain perpendicular to the tangential plane in the deformed configuration, yields

$$\boldsymbol{F}^{i\mathrm{T}} \cdot \boldsymbol{d}^i = 0 \quad \text{and} \quad \boldsymbol{d}^i \cdot \boldsymbol{F}^i = 0, \qquad (i = 1, 2) \text{ with } \boldsymbol{F}^{i\mathrm{T}} = \nabla_2 \otimes \boldsymbol{x}^i = \boldsymbol{a}^\alpha \otimes \frac{\partial \boldsymbol{x}^i}{\partial q^\alpha} = \boldsymbol{a}^\alpha \otimes \boldsymbol{g}^i_\alpha. \tag{11}$$

The tangential vectors $\boldsymbol{g}^i_\alpha$ define the tangential plane in the deformed configuration. The application of the in-plane nabla operator

$$\nabla_2 \otimes (\boldsymbol{F}^{i\mathrm{T}} \cdot \boldsymbol{d}^i) = \boldsymbol{0} = (\nabla_2 \otimes \boldsymbol{F}^{i\mathrm{T}}) \cdot \boldsymbol{d}^i + (\nabla_2 \otimes \boldsymbol{d}^i) \cdot \boldsymbol{F}^i$$

at first yields to

$$\underline{\underline{(\nabla_2 \otimes \boldsymbol{d}^i) \cdot \boldsymbol{F}^i}} = -(\nabla_2 \otimes \boldsymbol{F}^{i\mathrm{T}}) \cdot \boldsymbol{d}^i = \underline{-(\nabla_2 \otimes \nabla_2 \otimes \boldsymbol{x}^i) \cdot \boldsymbol{d}^i}. \tag{12}$$

Taking into account that the bending strain Schoop (1988, 1999) for the ith skin is described by

$$\boldsymbol{\kappa}^i = \frac{1}{2}\left\{\boldsymbol{F}^{i\mathrm{T}} \cdot (\boldsymbol{d}^i \otimes \nabla_2) + \underline{\underline{(\nabla_2 \otimes \boldsymbol{d}^i) \cdot \boldsymbol{F}^i}}\right\} \tag{13}$$

and due to the consideration of the Kirchhoff-Hypothesis (Label: $\langle K \rangle$), the twice-underscored part in (13) can be found again in (12) and replaced by the underscored term of (12). Finally, after an analogous procedure for the transposed term (11) follows:

$$\overset{\langle K\rangle^i}{\boldsymbol{\kappa}} = -\frac{1}{2}\{\boldsymbol{d}^i\cdot(\boldsymbol{x}^i\otimes\nabla_2\otimes\nabla_2)+(\nabla_2\otimes\nabla_2\otimes\boldsymbol{x}^i)\cdot\boldsymbol{d}^i\}. \tag{14}$$

Taking (4) into account and approximate $\boldsymbol{d}^i$ by $\boldsymbol{d}$, which becomes less accurate in case of increasing shear deformations, finally the bending strain of the ith skin can be found

$$\overset{\langle K\rangle^i}{\boldsymbol{\kappa}} = -\frac{1}{2}\left\{\boldsymbol{d}\cdot(\boldsymbol{r}\otimes\nabla_2\otimes\nabla_2)+(\nabla_2\otimes\nabla_2\otimes\boldsymbol{r})\cdot\boldsymbol{d}\pm\frac{d}{2}[\boldsymbol{d}\cdot(\boldsymbol{d}\otimes\nabla_2\otimes\nabla_2)+(\nabla_2\otimes\nabla_2\otimes\boldsymbol{d})\cdot\boldsymbol{d}]\right\}. \tag{15}$$

2.2.4. The stress resultans of SW-skins

As resultants of the second Piola–Kirchhoff stresses $\boldsymbol{S}^i = S^{i\alpha\beta}\boldsymbol{a}_\alpha\otimes\boldsymbol{a}_\beta$ over the skin thickness t, the second PK-skin membrane and skin moment tensors are defined as follows:

$$\boldsymbol{n}^i = \int_{z^i=0}^{t}\boldsymbol{S}^i\,\mathrm{d}z^i \quad \text{and} \quad \boldsymbol{m}^i = \int_{z^i=0}^{t} z^i\boldsymbol{S}^i\,\mathrm{d}z^i, \qquad (i=1,2). \tag{16}$$

2.2.5. The midsurface related SW-quantities

In order to achieve clarity as well as a better comparability regarding the SWMT, all quantities are related to the midsurface. Furthermore, the stress resultants which correspond to the SWMT $(\boldsymbol{N},\boldsymbol{M},\boldsymbol{Q})$ are labeled by capital letters. From the consideration of the skins according to Figs. 4–7 the 2nd Piola–Kirchhoff stress resultants and the Green–Lagrangian strain SW-quantities can be specified:

- SW-membrane force and SW-membrane strain tensor (see (10) and (16))

$$\boldsymbol{N} = \boldsymbol{n}^1 + \boldsymbol{n}^2, \tag{17}$$

$$\boldsymbol{D} = \frac{1}{2}(\boldsymbol{D}^1+\boldsymbol{D}^2) = \frac{1}{2}\left[\boldsymbol{F}^{\mathrm{T}}\cdot\boldsymbol{F}-\boldsymbol{E}_2+\frac{d^2}{4}\boldsymbol{G}^{\mathrm{T}}\cdot\boldsymbol{G}\right]. \tag{18}$$

- SW-moment and SW-bending strain tensor (see (10) and (16))

$$\boldsymbol{M} = \frac{d}{2}(\boldsymbol{n}^1-\boldsymbol{n}^2) \tag{19}$$

$$\boldsymbol{\kappa} = \frac{1}{d}(\boldsymbol{D}^1-\boldsymbol{D}^2) = \frac{1}{2}(\boldsymbol{F}^{\mathrm{T}}\cdot\boldsymbol{G}+\boldsymbol{G}^{\mathrm{T}}\cdot\boldsymbol{F}), \tag{20}$$

respectively for recalculation

$$\left(\boldsymbol{n}^{1,2} = \frac{1}{2}\boldsymbol{N}\pm\frac{1}{d}\boldsymbol{M};\ \boldsymbol{D}^{1,2} = \boldsymbol{D}\pm\frac{d}{2}\boldsymbol{\kappa}\right). \tag{21}$$

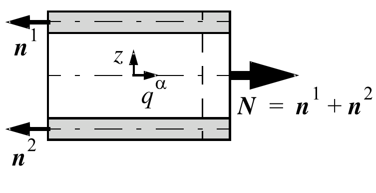

Fig. 4. Membrane force.

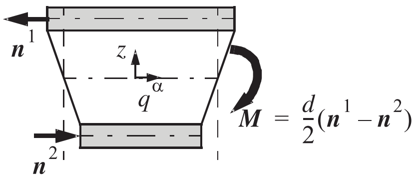

Fig. 5. (Membrane-) moment.

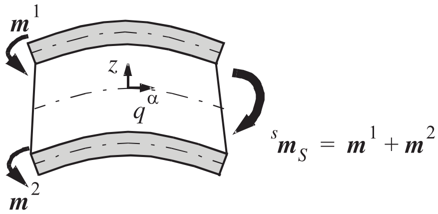

Fig. 6. Sum skin moment.

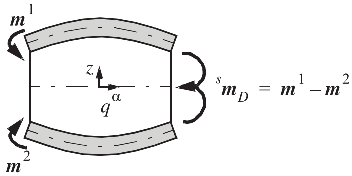

Fig. 7. Difference skin moment.

- Sum of SW-skin bending moment and SW-skin bending strain tensor (see (14) and (16))

$$ {}^{\mathrm{s}}\boldsymbol{m}_{\mathrm{S}} = \boldsymbol{m}^1 + \boldsymbol{m}^2 \tag{22}$$

$$ \overset{\langle K\rangle}{\boldsymbol{\kappa}}_{\mathrm{S}} = \tfrac{1}{2}\left(\overset{\langle K\rangle}{\boldsymbol{\kappa}}{}^1 + \overset{\langle K\rangle}{\boldsymbol{\kappa}}{}^2\right) = -\frac{1}{2}\{\boldsymbol{d}\cdot(\boldsymbol{r}\otimes\boldsymbol{\nabla}_2\otimes\boldsymbol{\nabla}_2) + (\boldsymbol{\nabla}_2\otimes\boldsymbol{\nabla}_2\otimes\boldsymbol{r})\cdot\boldsymbol{d}\} \tag{23}$$

- SW-skin bending moment and SW-skin bending strain difference-tensor (see (14) and (16))

$$ {}^{\mathrm{s}}\boldsymbol{m}_{\mathrm{D}} = \boldsymbol{m}^1 - \boldsymbol{m}^2, \tag{24}$$

$$ \overset{\langle K\rangle}{\boldsymbol{\kappa}}_{\mathrm{D}} = \frac{1}{2}\left(\overset{\langle K\rangle}{\boldsymbol{\kappa}}{}^1 - \overset{\langle K\rangle}{\boldsymbol{\kappa}}{}^2\right) = -\frac{1}{2}\left\{\frac{d}{2}[\boldsymbol{d}\cdot(\boldsymbol{d}\otimes\boldsymbol{\nabla}_2\otimes\boldsymbol{\nabla}_2) + (\boldsymbol{\nabla}_2\otimes\boldsymbol{\nabla}_2\otimes\boldsymbol{d})\cdot\boldsymbol{d}]\right\}, \tag{25}$$

respectively, for recalculation

$$ \left(\boldsymbol{m}^{1,2} = \frac{1}{2}({}^{\mathrm{s}}\boldsymbol{m}_{\mathrm{S}} \pm {}^{\mathrm{s}}\boldsymbol{m}_{\mathrm{D}});\ \overset{\langle K\rangle}{\boldsymbol{\kappa}}{}^{1,2} = \overset{\langle K\rangle}{\boldsymbol{\kappa}}_{\mathrm{S}} \pm \overset{\langle K\rangle}{\boldsymbol{\kappa}}_{\mathrm{D}}\right). \tag{26}$$

From quantities presented above the virtual inner work of the SW-skins is obtained

$$ \delta^{\mathrm{s}}A_i = \int_A \left(\boldsymbol{N}\cdot\cdot\delta\boldsymbol{D} + \boldsymbol{M}\cdot\cdot\delta\boldsymbol{\kappa} + {}^{\mathrm{s}}\boldsymbol{m}_{\mathrm{S}}\cdot\cdot\delta\overset{\langle K\rangle}{\boldsymbol{\kappa}}_{\mathrm{S}} + {}^{\mathrm{s}}\boldsymbol{m}_{\mathrm{D}}\cdot\cdot\delta\overset{\langle K\rangle}{\boldsymbol{\kappa}}_{\mathrm{D}}\right)\mathrm{d}A, \tag{27}$$

where "$\cdot\cdot$" specifies the double contraction according to $N_{\alpha\beta}\delta D_{\beta\alpha}$.

2.3. Kinematic and static variables of the SW-core

2.3.1. The approach for core deformation

Different preliminary considerations have shown (Vonach and Rammerstorfer, 2000; Kühhorn, 1991; Golze, 2000) that the short-wave wrinkling problem, which appears mainly in the case of thin skins and thick core, requires an improved description of the SW-core concerning transversal, shear, and longitudinal stiffness. Therefore an extended kinematic approach for the core deformation in comparison to Kühhorn (1991, 1993) and Kühhorn and Schoop (1992) is developed which provides a quadratic thickness stretch and a linear shear strain each in z-direction, as well as a consideration of associated cross-section warping.

It should be mentioned that an approximation of the thickness strain distribution up to the quadratic order is still crude. Indeed numerical investigations using three-dimensional finite elements demonstrate that it may be more important to take the core warping into account than to expand the thickness strain distribution further.

The derivation of this compatible displacement field is, at first, realised for the SW-bar (Fig. 8) considering small displacements (first-order theory). Subsequently a generalisation with regard to geometric nonlinearity and multidimensionality is realised with the help of invariant expressions concerning the strains; the generalisation holds for large rotations but moderate core strains.

The approach is based on a displacement field $u(x,z)$ (longitudinal direction) and $w(x,z)$ (thickness direction) corresponding to Kühhorn (1991) and Golze (2000):

$$u(x,z) = C_{\mathrm{I}} + zC_{\mathrm{II}} + \left(z^2 - \frac{h^2}{4}\right)C_{\mathrm{III}} + z\left(z^2 - \frac{h^2}{4}\right)C_{\mathrm{IV}} + \left(z^2 - \frac{h^2}{4}\right)\left(z^2 - \frac{h^2}{2}\right)C_{\mathrm{V}}, \tag{28}$$

$$w(x,z) = w + z\alpha_{z0} + \left(z^2 - \frac{h^2}{4}\right)\frac{\alpha_{z1}}{h} + z\left(z^2 - \frac{h^2}{4}\right)\frac{\alpha_{z2}}{h^2/2}. \tag{29}$$

According to Fig. 8 and analogous to Section 2.2.5 the following kinematic quantities, defined with regard to the geometric centerline, are applied:

$$u(x) = \frac{u^1 + u^2}{2}, \quad w(x) = \frac{w^1 + w^2}{2}, \quad \alpha_{z1}(x), \tag{30}$$

$$\beta(x) = \frac{u^1 - u^2}{d}, \quad \alpha_{z0} = \frac{d}{h}\frac{w^1 - w^2}{d}, \quad \alpha_{z2}(x) \tag{31}$$

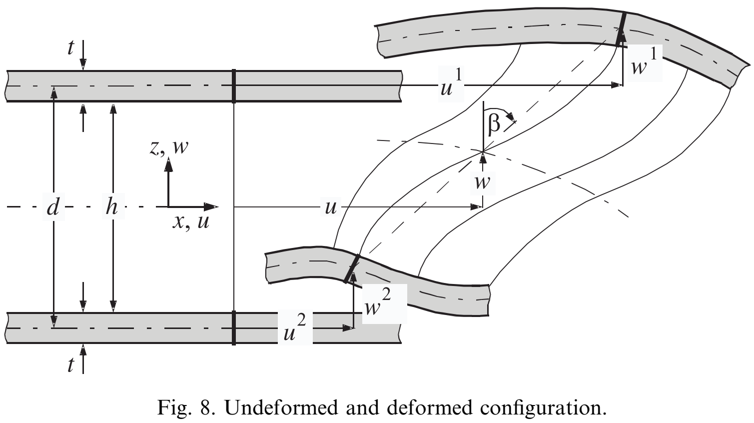

Fig. 8. Undeformed and deformed configuration.

and thus

$$u^i(x) = u \pm \frac{d}{2}\beta, \quad w^i(x) = w \pm h\alpha_{z0}. \tag{32}$$

Afterwards, the derivative of x will be marked by a dash

$$\frac{\partial}{\partial x}() = ()'. \tag{33}$$

The adjustment of (28) and (29) to the skin edges (Fig. 8) requires

$$u\left(x, z \pm \frac{h}{2}\right) = u^i \pm \frac{t}{2}(w^i)' \quad \text{and} \quad w\left(x, z \pm \frac{h}{2}\right) = w^i, \ \ (i = 1, 2) \tag{34}$$

where w^i in (34) is identically satisfied. Assuming that the shear strain distribution in thickness direction remains linear and the linear part depends exclusively on α_{z2}, the determination of the remaining constants becomes possible, and from this the compatible displacement- and strain fields become (see also Fig. 9):

$$\begin{array}{lcccccccc}
u(x,z) & = & u + z\frac{d}{h}\left(\beta + \frac{t}{d}w'\right) & + & g_0(z^2)\alpha'_{z0} & + & g_1(z^3)\alpha'_{z1} & + & g_2(z^4)\alpha'_{z2} \\
 & \| & & & \| & & \| & & \| \\
w(x,z) & = & w & + & z\alpha_{z0} & + & \left(z^2 - \frac{h^2}{4}\right)\frac{\alpha_{z1}}{h} & + & z\left(z^2 - \frac{h^2}{4}\right)\frac{\alpha_{z2}}{h^2/2} \\
 & \| & & & \| & & \| & & \| \\
\varepsilon_{xx} = \frac{\partial u}{\partial x} & = & u' + z\frac{d}{h}\left(\beta' + \frac{t}{d}w''\right) & + & g_0(z^2)\alpha''_{z0} & + & g_1(z^3)\alpha''_{z1} & + & g_2(z^4)\alpha''_{z2} \\
 & \| & & & \| & & \| & & \| \\
\varepsilon_{zz} = \frac{\partial w}{\partial z} & = & 0 & + & \alpha_{z0} & + & \frac{z}{h/2}\alpha_{z1} & + & \left(\frac{z^2}{h^2/6} - \frac{1}{2}\right)\alpha_{z2} \\
 & \| & & & \| & & \| & & \| \\
\varepsilon_{xz} = \frac{\left(\frac{\partial u}{\partial z} + \frac{\partial w}{\partial x}\right)}{2} & = & \frac{d}{2h}(\beta + w') & + & 0 & + & \left(-\frac{h}{12}\right)\alpha'_{z1} & + & \frac{z}{8}\alpha'_{z2} \\
 & \| & & & \| & & \| & & \| \\
\text{Parts}: & & \leftarrow \boldsymbol{A} \rightarrow & & \leftarrow \boldsymbol{B} \rightarrow & & \leftarrow \boldsymbol{C} \rightarrow & & \leftarrow \boldsymbol{D} \rightarrow
\end{array} \tag{35}$$

with the warping functions

$$\begin{aligned}
g_0(z^2) &= \frac{1}{2}\left[\frac{th}{2} + \left(\frac{h^2}{4} - z^2\right)\right], \\
g_1(z^3) &= \frac{z}{3h}\left(\frac{h^2}{4} - z^2\right), \\
g_2(z^4) &= \frac{1}{2h^2}\left(\frac{h^2}{4} - z^2\right)\left(z^2 - \frac{h^2}{2}\right).
\end{aligned} \tag{36}$$

α_{z0}, α_{z1}, α_{z2} are intensity coefficients corresponding to the weighted constant, linear, and quadratic parts of the thickness stretch ε_{zz} in (35). These intensity coefficients are treated as additional kinematic degrees of freedom. Fig. 9 shows the separated parts of the core warping according to (35), where A corresponds to the Timoshenko- and Reissner/Mindlin-part of the SWMT, whereas the parts ***B***, ***C*** and ***D*** are new and provide reasons for the improved core description. In Fig. 10 some combinations of symmetric parts of the deformations ***B*** and ***C*** as well as the antimetric parts ***A*** and ***D*** are exemplarily shown with regard to their appearance in case of a local loss of stability due to wrinkling waves. A generalisation in terms of nonlinear Green–Lagrangian strains corresponds to Kühhorn (1991, 1993) and Kühhorn and Schoop (1992) by describing the strain quantities in a coordinate-invariant way using eight SW-DOF $\boldsymbol{r}$, $\boldsymbol{d}$, α_{z1}, α_{z2} and the quantities of (18), (20), (23), (36) as follows:

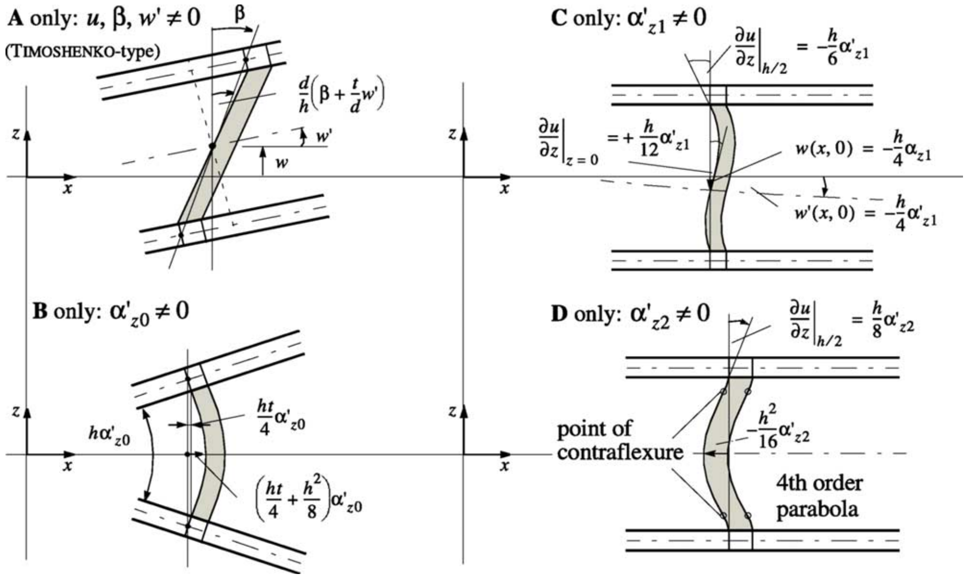

Fig. 9. Contribution of warping in (35).

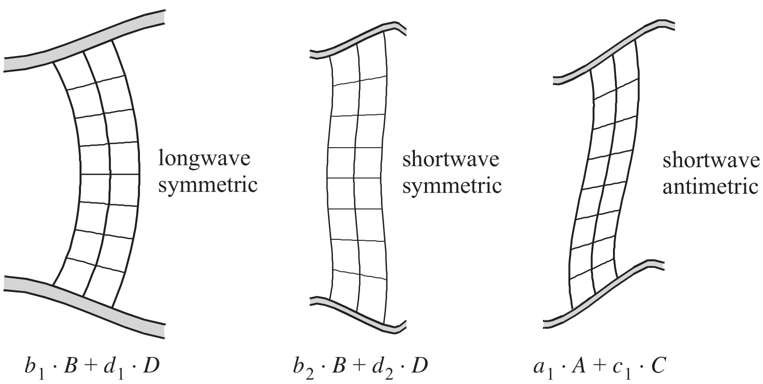

Fig. 10. Combinations of core deformation parts.

$$ {}^{\mathrm{c}}\boldsymbol{D}(q^{\alpha},z) = {}^{\mathrm{c}}\boldsymbol{D}_0 + z\frac{d}{h}\left(\boldsymbol{\kappa} - \frac{t}{d}\overset{\langle K\rangle}{\boldsymbol{\kappa}}_{\mathrm{S}}\right) + \sum_{i=0}^{2} g(z^{i+2})_i \boldsymbol{\nabla}_2 \otimes \boldsymbol{\nabla}_2 \alpha_{zi}, \tag{37} $$

$$ {}^{\mathrm{c}}\varepsilon_{zz}(q^{\alpha},z) = \alpha_{z0} + \frac{z}{h/2}\alpha_{z1} + \left(\frac{z^2}{h^2/6} - \frac{1}{2}\right)\alpha_{z2}, \tag{38} $$

$$ {}^{\mathrm{c}}\boldsymbol{e}_s(q^{\alpha},z) = \frac{d}{2h}\left(\boldsymbol{F}^{\mathrm{T}} \cdot \boldsymbol{d} - \frac{h^2}{6d}\boldsymbol{\nabla}_2\alpha_{z1}\right) + \frac{z}{8}\boldsymbol{\nabla}_2\alpha_{z2}, \tag{39} $$

where

$$^{c}\boldsymbol{D}_0 = \frac{1}{2}(\boldsymbol{F}^{\mathrm{T}} \cdot \boldsymbol{F} - \boldsymbol{E}_2) \quad \text{and} \quad \alpha_{z0} = \frac{d}{2h}(\boldsymbol{d} \cdot \boldsymbol{d} - 1). \tag{40}$$

The three-dimensional Green–Lagrangian strain tensor for the description of the core thus consists of an in-plane part (37), a part from thickness stretch (39), and finally, parts from transversal strains (38)

$$^{c}\boldsymbol{D}^{E3}(q^{\alpha}, z) = {}^{c}\boldsymbol{D} + {}^{c}\boldsymbol{e}_s \otimes \boldsymbol{n} + \boldsymbol{n} \otimes {}^{c}\boldsymbol{e}_s + {}^{c}\varepsilon_{zz}\boldsymbol{n} \otimes \boldsymbol{n}. \tag{41}$$

Therefore the kinematics of the core are valid for arbitrarily large rotations and displacements while the core strains should remain moderate, which is always given in the case of real SW-structures.

2.3.2. The arranged SW-core strains

Afterwards the core strains (37)–(39) are arranged in powers of z. Using (41) according to

$$^{c}\boldsymbol{D}^{E3}(q^{\alpha}, z) = \sum_{\ell=0}^{n} z^{\ell} \overset{\langle\ell\rangle}{\boldsymbol{D}}(q^{\alpha}), \tag{42}$$

the in-plane contribution (37) is obtained as

$$\begin{aligned}
&^{c}\boldsymbol{D} = \sum_{\ell=0}^{4} z^{\ell}\,{}^{c}\overset{\langle\ell\rangle}{\boldsymbol{D}}, \quad \text{with} \\
&^{c}\overset{\langle 0\rangle}{\boldsymbol{D}} = {}^{c}\boldsymbol{D}_0 + \left(\frac{th}{4} + \frac{h^2}{8}\right)\boldsymbol{\nabla}_2 \otimes \boldsymbol{\nabla}_2\alpha_{z0} - \frac{h^2}{16}\boldsymbol{\nabla}_2 \otimes \boldsymbol{\nabla}_2\alpha_{z2}, \\
&^{c}\overset{\langle 1\rangle}{\boldsymbol{D}} = \frac{d}{h}\left(\boldsymbol{\kappa} - \frac{t}{d}\overset{\langle K\rangle}{\boldsymbol{\kappa}}\right) + \frac{h}{12}\boldsymbol{\nabla}_2 \otimes \boldsymbol{\nabla}_2\alpha_{z1}, \\
&^{c}\overset{\langle 2\rangle}{\boldsymbol{D}} = -\frac{1}{2}\boldsymbol{\nabla}_2 \otimes \boldsymbol{\nabla}_2\alpha_{z0} + \frac{3}{8}\boldsymbol{\nabla}_2 \otimes \boldsymbol{\nabla}_2\alpha_{z2}, \\
&^{c}\overset{\langle 3\rangle}{\boldsymbol{D}} = -\frac{1}{3h}\boldsymbol{\nabla}_2 \otimes \boldsymbol{\nabla}_2\alpha_{z1}, {}^{c}\overset{\langle 4\rangle}{\boldsymbol{D}} = -\frac{1}{2h^2}\boldsymbol{\nabla}_2 \otimes \boldsymbol{\nabla}_2\alpha_{z2},
\end{aligned} \tag{43}$$

the shear contribution (39) as

$$^{c}\boldsymbol{e}_s = \sum_{\ell=0}^{1} z^{\ell}\,{}^{c}\overset{\langle\ell\rangle}{\boldsymbol{e}}_s, \quad \text{where } {}^{c}\overset{\langle 0\rangle}{\boldsymbol{e}}_s = \frac{d}{2h}\left(\boldsymbol{F} \cdot \boldsymbol{d} - \frac{h^2}{6d}\boldsymbol{\nabla}_2\alpha_{z1}\right), \ {}^{c}\overset{\langle 1\rangle}{\boldsymbol{e}}_s = \frac{1}{8}\boldsymbol{\nabla}_2\alpha_{z2} \tag{44}$$

and the transversal contribution (38) as

$$^{c}\varepsilon_{zz} = \sum_{\ell=0}^{2} z^{\ell}\,{}^{c}\overset{\langle\ell\rangle}{\varepsilon}_{zz}, \quad \text{where } {}^{c}\overset{\langle 0\rangle}{\varepsilon}_{zz} = \alpha_{z0} - \frac{1}{2}\alpha_{z2}, \ {}^{c}\overset{\langle 1\rangle}{\varepsilon}_{zz} = \frac{2}{h}\alpha_{z1}, \ {}^{c}\overset{\langle 2\rangle}{\varepsilon}_{zz} = \frac{6}{h^2}\alpha_{z2}. \tag{45}$$

2.3.3. Definition of SW-core stress resultants

The stress resultants are defined systematically corresponding to

$$^{c}\overset{\langle\ell\rangle}{\boldsymbol{s}} = \int_{z=-h/2}^{z=+h/2} z^{\ell}\,{}^{c}\boldsymbol{S}\,\mathrm{d}z \quad \text{and} \quad \ell = 0, 1, \ldots, \tag{46}$$

where $\ell = 0, 1, 2, \ldots$ indicates the parts from force, moment, bi-moment etc. Thus the in-plane core stress tensor resultants ($\ell = 1, 2, 3, 4$) are described as

$$
\begin{aligned}
&{}^{c}\overset{\langle\ell\rangle}{\boldsymbol{n}} = \int z^{\ell c}S_{\alpha\beta}\,\mathrm{d}z\boldsymbol{e}_\alpha \otimes \boldsymbol{e}_\beta, \quad \text{where} \\
&{}^{c}\overset{\langle 0\rangle}{\boldsymbol{n}} = {}^{c}\boldsymbol{n}, \quad {}^{c}\overset{\langle 1\rangle}{\boldsymbol{n}} = {}^{c}\boldsymbol{m} \quad \text{(core-membrane force and-bending moment)}, \\
&{}^{c}\overset{\langle 2\rangle}{\boldsymbol{n}}, {}^{c}\overset{\langle 3\rangle}{\boldsymbol{n}}, {}^{c}\overset{\langle 4\rangle}{\boldsymbol{n}} \quad \text{(bi-, tri-, quatro-moment)}.
\end{aligned}
\tag{47}
$$

The shear vector resultants ($\ell = 0, 1$) are

$$
\begin{aligned}
&{}^{c}\overset{\langle\ell\rangle}{\boldsymbol{Q}} = \int z^{\ell c}S_{z\alpha}\,\mathrm{d}z\boldsymbol{e}_\alpha, \quad \text{where} \\
&{}^{c}\overset{\langle 0\rangle}{\boldsymbol{Q}} = {}^{c}\boldsymbol{Q}, {}^{c}\overset{\langle 1\rangle}{\boldsymbol{Q}} \quad \text{(core-shear force and moment)}
\end{aligned}
\tag{48}
$$

and the transversal resultants ($\ell = 0, 1, 2$) are

$$
\begin{aligned}
&{}^{c}\overset{\langle\ell\rangle}{t} = \int z^{\ell c}S_{zz}\,\mathrm{d}z, \quad \text{where} \\
&{}^{c}\overset{\langle 0\rangle}{t}, {}^{c}\overset{\langle 1\rangle}{t}, {}^{c}\overset{\langle 2\rangle}{t} \quad \text{(transversal force, moment, and bi-moment)}.
\end{aligned}
\tag{49}
$$

For a clear arrangement the expressions ${}^{c}\overset{\langle 0\rangle}{\boldsymbol{n}}$, ${}^{c}\overset{\langle 1\rangle}{\boldsymbol{n}}$, ${}^{c}\overset{\langle 0\rangle}{\boldsymbol{Q}}$ are simplified to ${}^{c}\boldsymbol{n}$, ${}^{c}\boldsymbol{m}$, ${}^{c}\boldsymbol{Q}$.

Thus the virtual inner work of the SW-core can easily be formulated as:

$$
\delta^{c}A_i = \int_A \left(\sum_{\ell=0}^{4} {}^{c}\overset{\langle\ell\rangle}{\boldsymbol{n}} \cdot\cdot\, \delta^{c}\overset{\langle\ell\rangle}{\boldsymbol{D}} + \sum_{\ell=0}^{1} 2^{c}\overset{\langle\ell\rangle}{\boldsymbol{Q}} \cdot \delta^{c}\overset{\langle\ell\rangle}{\boldsymbol{e}}_s + \sum_{\ell=0}^{2} {}^{c}\overset{\langle\ell\rangle}{t}\,\delta^{c}\overset{\langle\ell\rangle}{\varepsilon}_{zz} \right) \mathrm{d}A. \tag{50}
$$

2.4. The external loads

The total virtual external work due to boundary (see 2.5), surface and volume loads has to be split up according to

$$
\delta A_e = \delta A_b + \delta A_{es} + \delta A_{ev}. \tag{51}
$$

As simplification, volume forces are neglected (else see Kühhorn, 1991), and surface forces $\boldsymbol{p}^i(q^\alpha)$ are related to the skin midsurfaces (Fig. 11). The result is:

$$
\delta A_{es} = \int_A (\boldsymbol{p}^1 \cdot \delta\boldsymbol{x}^1 + \boldsymbol{p}^2 \cdot \delta\boldsymbol{x}^2)\mathrm{d}A = \int (\boldsymbol{p}_0 \cdot \delta\boldsymbol{r} + \boldsymbol{p}_1 \cdot \delta\boldsymbol{d})\mathrm{d}A \tag{52}
$$

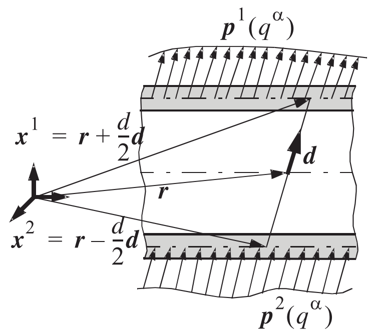

Fig. 11. Surface loads.

in which

$$\boldsymbol{p}_0 = \boldsymbol{p}^1 + \boldsymbol{p}^2 \quad \text{and} \quad \boldsymbol{p}_1 = \frac{d}{2}(\boldsymbol{p}^1 - \boldsymbol{p}^2) \tag{53}$$

are external surface force and force couple vectors.

2.5. Equilibrium and boundary conditions

2.5.1. Principle of virtual work on the SW-structure

The deduction is based on the principle of virtual work:

$$\delta A_e = \delta A_i \Longleftrightarrow \delta A_b + \delta A_{es} = \delta^{\mathrm{s}} A_i + \delta^{\mathrm{c}} A_i, \tag{54}$$

specified by (27), (50), (52) to the above SW-structure

$$\delta A_b + \int_A (\boldsymbol{p}_0 \cdot \delta \boldsymbol{r} + \boldsymbol{p}_1 \cdot \delta \boldsymbol{d}) \mathrm{d}A = \int_A \Bigg\{ \Bigg(\boldsymbol{N} \cdot\cdot \delta \boldsymbol{D} + \boldsymbol{M} \cdot\cdot \delta \boldsymbol{\kappa} + {}^{\mathrm{s}}\boldsymbol{m}_{\mathrm{S}} \cdot\cdot \delta \overset{\langle K \rangle}{\boldsymbol{\kappa}}_{\mathrm{S}} + {}^{\mathrm{s}}\boldsymbol{m}_{\mathrm{D}} \cdot\cdot \delta \overset{\langle K \rangle}{\boldsymbol{\kappa}}_{\mathrm{D}} \Bigg) + \Bigg(\sum_{p=0}^{4} {}^{\mathrm{c}}\overset{\langle p \rangle}{\boldsymbol{n}} \cdot\cdot \delta^{\mathrm{c}} \overset{\langle p \rangle}{\boldsymbol{D}} + \sum_{p=0}^{1} 2^{\mathrm{c}} \overset{\langle p \rangle}{\boldsymbol{Q}} \cdot \delta^{\mathrm{c}} \overset{\langle p \rangle}{\boldsymbol{e}}_{\mathrm{S}} + \sum_{p=0}^{2} {}^{\mathrm{c}}\overset{\langle p \rangle}{t} \delta^{\mathrm{c}} \overset{\langle p \rangle}{\varepsilon}_{zz} \Bigg) \Bigg\} \mathrm{d}A \tag{55}$$

transformed by the use of Stoke's theorem

$$\int_A \boldsymbol{\nabla}_2 \odot \boldsymbol{\Phi} \, dA = \oint (\mathrm{d}\boldsymbol{R} \times \boldsymbol{n}) \odot \boldsymbol{\Phi} = \oint \boldsymbol{e}_\perp \odot \boldsymbol{\Phi} \, ds, \tag{56}$$

where $\odot$ is an arbitrary operation, $\boldsymbol{\Phi}$ a scalar, vectorial or tensorial term and $\boldsymbol{e}_\perp$ is the unit vector, normal to the boundary curve (Fig. 12). A structure such as

$$\delta A_i - \delta A_e = \underline{\oint \boldsymbol{e}_\perp \odot [\tilde{\boldsymbol{\Phi}}] \delta\psi \, \mathrm{d}s} - \int_A \boldsymbol{\nabla}_2 \odot [\tilde{\boldsymbol{\Phi}}] \delta\psi \, \mathrm{d}A \tag{57}$$

is formed, in which the underlined term (see Trostel, 1985, 1988) represents the boundary work, and the remaining term represents the Euler–Lagrange equations. Furthermore some terms appear such as

$$\oint \boldsymbol{e}_\perp \cdot (-{}^{\mathrm{s}}\boldsymbol{m}_{\mathrm{S}} \otimes \boldsymbol{d}) \cdot\cdot (\delta \boldsymbol{r} \otimes \boldsymbol{\nabla}_2) \mathrm{d}s, \tag{58}$$

which have to be additionally transformed in the sense of Thomson–Tait, because, in case of a variation of $\delta \boldsymbol{r}$, the part $\partial \boldsymbol{r}/\partial s$ at the boundary is already determined and has not been varied independently. Therefore the Nabla-Operator in (58) has to be rearranged in a part perpendicular and a part tangential to the edge curve

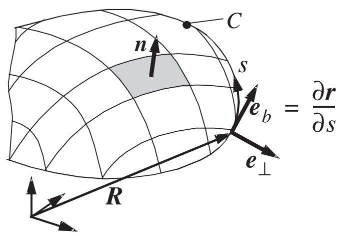

Fig. 12. Edge curve.

$$\nabla_2^b = \boldsymbol{e}_b \frac{\partial}{\partial s} + \boldsymbol{e}_\perp \frac{\partial}{\partial s_\perp}. \tag{59}$$

The term (58) has to be processed corresponding to (59) (see also Kühhorn, 1991).

2.5.2. The nonlinear equilibrium and boundary conditions

Subsequently, the quantities $\bar{\psi}$, which put together parts from the skin and the core, are marked with an overline, whereas combinations with core parts only are marked as $\tilde{\psi}$. Using the definitions (17), (19), (22), (24), (47), (48) and (49) the second Piola–Kirchhoff tensors are determined (see Figs. 4–7):

$$\overline{\boldsymbol{N}} = \boldsymbol{N} + {}^{\mathrm{c}}\boldsymbol{n}, \quad \overline{\boldsymbol{M}} = \boldsymbol{M} + \frac{d}{h}{}^{\mathrm{c}}\boldsymbol{m}, \tag{60}$$

$$\overline{\boldsymbol{m}}_{\mathrm{S}} = {}^{\mathrm{s}}\boldsymbol{m}_{\mathrm{S}} - \frac{t}{h}{}^{\mathrm{c}}\boldsymbol{m}, \quad \overline{\boldsymbol{m}}_{\mathrm{D}} = \frac{d}{2}{}^{\mathrm{s}}\boldsymbol{m}_{\mathrm{D}} - \frac{d}{h}\left(\frac{th}{4} + \frac{h^2}{8}\right){}^{\mathrm{c}}\boldsymbol{n} + \frac{d}{2h}{}^{\mathrm{c}}\overset{\langle 2\rangle}{\boldsymbol{n}}, \tag{61}$$

$$\tilde{\boldsymbol{n}} = \frac{h^2}{16}{}^{\mathrm{c}}\boldsymbol{n} - \frac{3}{8}{}^{\mathrm{c}}\overset{\langle 2\rangle}{\boldsymbol{n}} + \frac{1}{2h^2}{}^{\mathrm{c}}\overset{\langle 4\rangle}{\boldsymbol{n}}, \quad \tilde{\boldsymbol{m}} = -\frac{h}{12}{}^{\mathrm{c}}\boldsymbol{m} + \frac{1}{3h}{}^{\mathrm{c}}\overset{\langle 3\rangle}{\boldsymbol{n}} \tag{62}$$

as well as, the first Piola–Kirchhoff tensors, which are needed for the equilibrium conditions:

$$\overline{\boldsymbol{N}}^{1\mathrm{P}} = \overline{\boldsymbol{N}} \cdot \boldsymbol{F}^{\mathrm{T}} + \overline{\boldsymbol{M}} \cdot \boldsymbol{G}^{\mathrm{T}} + \nabla_2 \cdot (\overline{\boldsymbol{m}}_{\mathrm{S}} \otimes \boldsymbol{d}), \tag{63}$$

$$\overline{\boldsymbol{M}}^{1\mathrm{P}} = \overline{\boldsymbol{M}} \cdot \boldsymbol{F}^{\mathrm{T}} + \frac{d^2}{4}\boldsymbol{N} \cdot \boldsymbol{G}^{\mathrm{T}} + \nabla_2 \cdot (\overline{\boldsymbol{m}}_{\mathrm{D}} \otimes \boldsymbol{d}). \tag{64}$$

Corresponding to the variations $\delta\boldsymbol{r}$, $\delta\boldsymbol{d}$, $\delta\alpha_{z1}$, $\delta\alpha_{z2}$ the field equations for force, moment, and bi-moments equilibrium arise

$$\delta\boldsymbol{r}: \quad \nabla_2 \cdot \left(\overline{\boldsymbol{N}}^{1\mathrm{P}} + \frac{d}{h}{}^{\mathrm{c}}\boldsymbol{Q} \otimes \boldsymbol{d}\right) + \boldsymbol{p}_0 = \boldsymbol{0}, \tag{65}$$

$$\delta\boldsymbol{d}: \quad \nabla_2 \cdot (\overline{\boldsymbol{M}}^{1\mathrm{P}}) - \frac{d}{h}{}^{\mathrm{c}}\boldsymbol{Q} \cdot \boldsymbol{F}^{\mathrm{T}} - \frac{d}{h}{}^{\mathrm{c}}\overset{\langle 0\rangle}{t}\boldsymbol{d} + \overline{\boldsymbol{m}}_{\mathrm{S}} \cdot\cdot (\nabla_2 \otimes \nabla_2 \otimes \boldsymbol{r}) + \overline{\boldsymbol{m}}_{\mathrm{D}} \cdot\cdot (\nabla_2 \otimes \nabla_2 \otimes \boldsymbol{d}) + \boldsymbol{p}_1 = \boldsymbol{0}, \tag{66}$$

$$\delta\alpha_{z1}: \quad \nabla_2 \cdot \left(-\frac{h}{6}{}^{\mathrm{c}}\boldsymbol{Q} + \nabla_2 \cdot \tilde{\boldsymbol{m}}\right) - \frac{2}{h}{}^{\mathrm{c}}\overset{\langle 1\rangle}{t} = 0, \tag{67}$$

$$\delta\alpha_{z2}: \quad \nabla_2 \cdot \left(\frac{1}{4}{}^{\mathrm{c}}\overset{\langle 1\rangle}{\boldsymbol{Q}} + \nabla_2 \cdot \tilde{\boldsymbol{n}}\right) + \frac{1}{2}{}^{\mathrm{c}}\overset{\langle 0\rangle}{t} - \frac{6}{h^2}{}^{\mathrm{c}}\overset{\langle 2\rangle}{t} = 0, \tag{68}$$

including the associated boundary conditions

$$\begin{aligned} &\delta\boldsymbol{r}: \quad \boldsymbol{p}^b = \boldsymbol{e}_\perp \cdot \left(\overline{\boldsymbol{N}}^{1\mathrm{P}} + \frac{d}{h}{}^{\mathrm{c}}\boldsymbol{Q} \otimes \boldsymbol{d}\right) + \frac{\partial}{\partial s}(\overline{m}_{S_{\perp b}}\boldsymbol{d}) \\ &\frac{\partial\delta\boldsymbol{r}}{\partial s_\perp}: \quad \overline{\boldsymbol{m}}_{\mathrm{S}}^b = \boldsymbol{e}_\perp \otimes \boldsymbol{e}_\perp \cdot\cdot (-\overline{\boldsymbol{m}}_{\mathrm{S}} \otimes \boldsymbol{d}), \end{aligned} \tag{69}$$

$$\begin{aligned} &\delta\boldsymbol{d}: \quad \boldsymbol{m}^b = \boldsymbol{e}_\perp \cdot \overline{\boldsymbol{M}}^{1\mathrm{P}} + \frac{\partial}{\partial s}(\overline{m}_{D_{\perp b}}\boldsymbol{d}) \\ &\frac{\partial\delta\boldsymbol{d}}{\partial s_\perp}: \quad \overline{\boldsymbol{m}}_{\mathrm{D}}^b = \boldsymbol{e}_\perp \otimes \boldsymbol{e}_\perp \cdot\cdot (-\overline{\boldsymbol{m}}_{\mathrm{D}} \otimes \boldsymbol{d}), \end{aligned} \tag{70}$$

$$\begin{aligned} \delta\alpha_{z1}: \quad & {}^{c}q_{z1}^{b} = \boldsymbol{e}_{\perp}\cdot\left(-\frac{h}{6}{}^{c}\boldsymbol{Q}+\nabla_{2}\cdot\tilde{\boldsymbol{m}}\right)-\frac{\partial}{\partial s}(\tilde{m}_{\perp b}) \\ \frac{\partial\delta\alpha_{z1}}{\partial s_{\perp}}: \quad & -\tilde{m}_{\perp\perp}^{b} = \boldsymbol{e}_{\perp}\otimes\boldsymbol{e}_{\perp}\cdot\cdot(-\tilde{\boldsymbol{m}}), \end{aligned} \tag{71}$$

$$\begin{aligned} \delta\alpha_{z2}: \quad & {}^{c}m_{z2}^{b} = \boldsymbol{e}_{\perp}\cdot\left(\frac{1}{4}{}^{c}\overset{\langle 1\rangle}{\boldsymbol{Q}}+\nabla_{2}\cdot\tilde{\boldsymbol{n}}\right)-\frac{\partial}{\partial s}(\tilde{n}_{\perp b}) \\ \frac{\partial\delta\alpha_{z2}}{\partial s_{\perp}}: \quad & -\tilde{n}_{\perp\perp}^{b} = \boldsymbol{e}_{\perp}\otimes\boldsymbol{e}_{\perp}\cdot\cdot(-\tilde{\boldsymbol{n}}). \end{aligned} \tag{72}$$

In (69)–(72) the generalised Thomson–Tait (drilling-) contributions appear ($\partial/\partial s[\cdots]$), where the labelling "$\perp b$" of a quantity ψ has to be interpreted as $[\psi]_{\perp b} = \boldsymbol{e}_{\perp}\otimes\boldsymbol{e}_{b}\cdot\cdot[\psi]$. The first PK-tensors (63) and (64) and the expression ${}^{c}\boldsymbol{Q}\otimes\boldsymbol{d}$ are dyads (as well as $\boldsymbol{F}^{T}$ and $\boldsymbol{G}^{T}$), which are planar with respect to the undeformed and spatial with regard to the deformed configuration, according to an arbitrary, e.g. cartesian base. Thus the terms $\overline{\boldsymbol{m}}_{S}\otimes\boldsymbol{d}$ respectively, $\overline{\boldsymbol{m}}_{D}\otimes\boldsymbol{d}$ correspond to $[2\times3\times3]$ tensors of third-order. A comparison with Kühhorn (1991, 1993) and Kühhorn and Schoop (1992) clearly shows the extension due to consideration of the core warping (additional terms ${}^{c}\psi$ and the additional equation (68) due to the eighth DOF).

2.6. Remarks on material equations

Generally, arbitrary material equations are applicable for the determination of the second PK-stresses in the skins and in the core, whereas a plane stress state ("Φ_{pl}") with regard to the skins is required. Applying the hyperelastic SaintVenant–Kirchhoff law

$$\boldsymbol{S} = \overset{\langle 4\rangle}{\boldsymbol{C}}\cdot\cdot\boldsymbol{D}, \tag{73}$$

e.g., the particular case of isotropy for the second PK-stresses of the skins

$${}^{s}\boldsymbol{S}_{pl} = 2{}^{s}G\left({}^{s}\boldsymbol{D}+\frac{{}^{s}\nu}{1-{}^{s}\nu}(\mathrm{tr}{}^{s}\boldsymbol{D})\boldsymbol{E}_{pl}\right) \tag{74}$$

and the second PK-stresses in the core

$${}^{c}\boldsymbol{S} = 2{}^{c}G\left({}^{c}\boldsymbol{D}+\frac{{}^{c}\nu}{1-2{}^{c}\nu}(\mathrm{tr}{}^{c}\boldsymbol{D})\boldsymbol{E}\right)$$

are obtained, which allows the calculation of the corresponding stress resultants.

2.7. First-order theory for plane SW-structures

Considering a linearisation of the general non-linear theory, first-order equations are presented with regard to a cartesian coordinate system (Fig. 13).

2.7.1. Kinematics

According to the eight DOFs we introduce (see Figs. 13 and 8):

- the displacement vector (of the geometric midsurface)

$$\boldsymbol{u} = \boldsymbol{u}_{pl}+w\boldsymbol{e}_{z}\hat{=}[u,v,w] \quad \text{with } \boldsymbol{u}_{pl}\hat{=}[u,v], \tag{75}$$

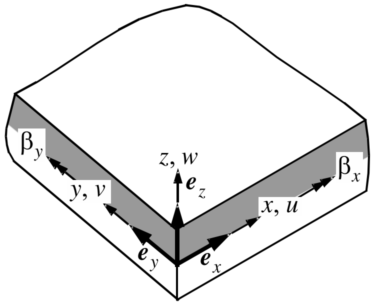

Fig. 13. Cartesian coordinates and base.

- the plane angular vector of the cross-section

$$\boldsymbol{\beta}_{\mathrm{pl}} \hat{=} [\beta_y, -\beta_x], \tag{76}$$

- the increase of director length e_3 and the intensity coefficients of the generalised thickness stretch (see (35) and Fig. 9)

$$e_3 = \frac{h}{d}\alpha_{z0}; \quad \alpha_{z1}; \quad \alpha_{z2}. \tag{77}$$

With

$$\begin{aligned} &\boldsymbol{r}^{\mathrm{I}} = \boldsymbol{R} + \boldsymbol{u}, \quad \boldsymbol{d}^{\mathrm{I}} = \boldsymbol{\beta}_{\mathrm{pl}} + (1 + e_3)\boldsymbol{e}_z, \\ &\boldsymbol{F}^{\mathrm{IT}} = \boldsymbol{\nabla}_2 \otimes \boldsymbol{u} + \nabla_2 \otimes \boldsymbol{R}, \quad \boldsymbol{G}^{\mathrm{IT}} = \boldsymbol{\nabla}_2 \otimes \boldsymbol{\beta}_{\mathrm{pl}} + (\boldsymbol{\nabla}_2 e_3) \otimes \boldsymbol{e}_z, \end{aligned} \tag{78}$$

the strains according to (18), (20), (22), (25) are

$$\boldsymbol{D}^{\mathrm{I}} = \frac{1}{2}(\boldsymbol{\nabla}_2 \otimes \boldsymbol{u}_{\mathrm{pl}} + \boldsymbol{u}_{\mathrm{pl}} \otimes \boldsymbol{\nabla}_2), \quad \boldsymbol{\kappa}^{\mathrm{I}} = \frac{1}{2}(\boldsymbol{\nabla}_2 \otimes \boldsymbol{\beta}_{\mathrm{pl}} + \boldsymbol{\beta}_{\mathrm{pl}} \otimes \boldsymbol{\nabla}_2), \tag{79}$$

$$\overset{\langle K \rangle}{\boldsymbol{\kappa}}{}^{\mathrm{I}}_{\mathrm{S}} = -\boldsymbol{\nabla}_2 \otimes \boldsymbol{\nabla}_2 w, \quad \overset{\langle K \rangle}{\boldsymbol{\kappa}}{}^{\mathrm{I}}_{\mathrm{D}} = -\frac{d}{2}\boldsymbol{\nabla}_2 \otimes \boldsymbol{\nabla}_2 e_3 \tag{80}$$

and to (43)–(45) or (37)–(39)

$${}^{\mathrm{c}}\boldsymbol{e}_s^{\mathrm{I}} = \frac{d}{2h}\left(\boldsymbol{\beta}_{\mathrm{pl}} + \boldsymbol{\nabla}_2 w - \frac{h^2}{6d}\boldsymbol{\nabla}_2 \alpha_{z1}\right) + \frac{z}{8}\boldsymbol{\nabla}_2 \alpha_{z2}, \tag{81}$$

$${}^{\mathrm{c}}\varepsilon_{zz}^{\mathrm{I}} = \frac{d}{h}e_3 - \frac{1}{2}\alpha_{z2} + \frac{z}{h/2}\alpha_{z1} + \frac{z^2}{h^2/6}\alpha_{z2}, \tag{82}$$

$${}^{\mathrm{c}}\boldsymbol{D}^{\mathrm{I}} = \sum_{\ell=0}^{4} z^{\ell}\,{}^{\mathrm{c}}\overset{\langle \ell \rangle}{\boldsymbol{D}}{}^{\mathrm{I}} \quad \text{with } {}^{\mathrm{c}}\overset{\langle \ell \rangle}{\boldsymbol{D}}{}^{\mathrm{I}} \text{by}(43). \tag{83}$$

2.7.2. Material laws

In general, an arbitrary constitutive law can be used for the core, whereas for the skins a constitutive law according to the assumed plane stress state has to be applied. From the use of Hooke's law (Kühhorn and Silber, 2000) the (planar) skin stress resultants

$$\begin{aligned}\boldsymbol{N} &= 2^{\mathrm{s}}G2t\left[\boldsymbol{D}^{\mathrm{I}} + \frac{{}^{\mathrm{s}}\nu}{1-{}^{\mathrm{s}}\nu}\operatorname{tr}\boldsymbol{D}^{\mathrm{I}}\boldsymbol{E}\right],\\ \boldsymbol{M} &= 2^{\mathrm{s}}G\frac{\mathrm{td}^2}{2}\left[\boldsymbol{\kappa}^{\mathrm{I}} + \frac{{}^{\mathrm{s}}\nu}{1-{}^{\mathrm{s}}\nu}\operatorname{tr}\boldsymbol{\kappa}^{\mathrm{I}}\boldsymbol{E}\right],\end{aligned} \tag{84}$$

$$\begin{aligned}{}^{\mathrm{s}}\boldsymbol{m}_{\mathrm{S}} &= 4^{\mathrm{s}}G\frac{t^3}{12}\left[\overset{\langle K\rangle}{\boldsymbol{\kappa}_{\mathrm{S}}}^{\mathrm{I}} + \frac{{}^{\mathrm{s}}\nu}{1-{}^{\mathrm{s}}\nu}\operatorname{tr}\overset{\langle K\rangle}{\boldsymbol{\kappa}_{\mathrm{S}}}^{\mathrm{I}}\boldsymbol{E}\right],\\ {}^{\mathrm{s}}\boldsymbol{m}_{\mathrm{D}} &= 4^{\mathrm{s}}G\frac{t^3}{12}\left[\overset{\langle K\rangle}{\boldsymbol{\kappa}_{\mathrm{D}}}^{\mathrm{I}} + \frac{{}^{\mathrm{s}}\nu}{1-{}^{\mathrm{s}}\nu}\operatorname{tr}\overset{\langle K\rangle}{\boldsymbol{\kappa}_{\mathrm{D}}}^{\mathrm{I}}\boldsymbol{E}\right]\end{aligned} \tag{85}$$

and the core stresses (3-dimensional) arise, considering (41):

$${}^{\mathrm{c}}\boldsymbol{S} = 2^{\mathrm{c}}G\left[{}^{\mathrm{c}}\boldsymbol{D}^{E3^{\mathrm{I}}} + \frac{{}^{\mathrm{c}}\nu}{1-2^{\mathrm{c}}\nu}tr^{\mathrm{c}}\boldsymbol{D}^{E3^{\mathrm{I}}}\boldsymbol{E}\right]. \tag{86}$$

2.7.3. The equilibrium and boundary conditions

In first-order theory the equilibrium conditions are formulated with regard to the undeformed configuration. Applying the equations of Section 2.5.2 it has to be noted that

$$\boldsymbol{F} \Rightarrow \boldsymbol{E}_2, \boldsymbol{G} \Rightarrow \overset{\langle 2\rangle}{\boldsymbol{0}}, \quad \boldsymbol{d} \Rightarrow \boldsymbol{e}_z, \quad \boldsymbol{\nabla}_2 \otimes \boldsymbol{\nabla}_2 \otimes \boldsymbol{r} \Rightarrow \overset{\langle 3\rangle}{\boldsymbol{0}}, \quad \boldsymbol{\nabla}_2 \otimes \boldsymbol{\nabla}_2 \otimes \boldsymbol{d} \Rightarrow \overset{\langle 3\rangle}{\boldsymbol{0}}$$

and that

$$\overline{\boldsymbol{N}}^{1\mathrm{P}} = \overline{\boldsymbol{N}} + \boldsymbol{\nabla}_2 \cdot \bar{\boldsymbol{m}}_{\mathrm{S}} \otimes \boldsymbol{e}_z, \quad \overline{\boldsymbol{M}}^{1\mathrm{P}} = \overline{\boldsymbol{M}} + \boldsymbol{\nabla}_2 \cdot \bar{\boldsymbol{m}}_{\mathrm{D}} \otimes \boldsymbol{e}_z \tag{87}$$

has to be set. The equilibrium and boundary conditions of the first-order theory can be clearly splitted using the forms (60)–(62) in parts which are symmetric and antimetric with reference to the midsurface:

- symmetric part (contains the disk problem) of the equilibrium conditions

$$\delta\boldsymbol{u}_{\mathrm{pl}}: \quad \boldsymbol{\nabla}_2 \cdot \overline{\boldsymbol{N}} + \boldsymbol{p}_{0_{\mathrm{pl}}} = 0 \tag{88}$$

$$\delta e_3: \quad \boldsymbol{\nabla}_2 \cdot \boldsymbol{\nabla}_2 \cdot \bar{\boldsymbol{m}}_{\mathrm{D}} - \frac{d}{h}{}^{\mathrm{c}}\overset{\langle 0\rangle}{t} + p_{1z} = 0, \tag{89}$$

$$\delta\alpha_{z2}: \quad \boldsymbol{\nabla}_2 \cdot \left(\frac{1}{4}{}^{\mathrm{c}}\overset{\langle 1\rangle}{\boldsymbol{Q}} + \boldsymbol{\nabla}_2 \cdot \tilde{\boldsymbol{n}}\right) + \frac{1}{2}{}^{\mathrm{c}}\overset{\langle 0\rangle}{t} - \frac{6}{h^2}{}^{\mathrm{c}}\overset{\langle 2\rangle}{t} = 0 \tag{90}$$

  and the boundary conditions

$$\delta\boldsymbol{u}_{\mathrm{pl}}: \quad \boldsymbol{p}^b_{\mathrm{pl}} = \boldsymbol{e}_\perp \cdot \overline{\boldsymbol{N}}, \tag{91}$$

$$\delta e_3: \quad m^b_3 = \boldsymbol{e}_\perp \cdot \boldsymbol{\nabla}_2 \cdot \overline{\boldsymbol{m}}_{\mathrm{D}}, \tag{92}$$

$$\frac{\partial\delta e_3}{\partial s_\perp}: \quad -\bar{m}^b_{\mathrm{D}} = -\bar{m}_{D_{\perp\perp}}, \tag{93}$$

$$\delta\alpha_{z2}: \quad {}^{\mathrm{c}}m^b_{z2} = \boldsymbol{e}_\perp \cdot \left(\frac{1}{4}{}^{\mathrm{c}}\overset{\langle 1\rangle}{\boldsymbol{Q}} + \boldsymbol{\nabla}_2 \cdot \tilde{\boldsymbol{n}}\right) - \frac{\partial}{\partial s}\tilde{n}_{\perp b}, \tag{94}$$

$$\frac{\partial \delta \alpha_{z2}}{\partial s_\perp}: \quad -\tilde{n}^b_{\perp\perp} = -\tilde{n}_{\perp\perp}; \tag{95}$$

- antimetric part (contains the plate problem) of the equilibrium conditions

$$\delta w: \quad \nabla_2 \cdot \left(\frac{d}{h}{}^{c}\boldsymbol{Q} + \nabla_2 \cdot \bar{\boldsymbol{m}}_S\right) + p_{0z} = 0, \tag{96}$$

$$\delta \boldsymbol{\beta}_{pl}: \quad \nabla_2 \cdot \overline{\boldsymbol{M}} - \frac{d}{h}{}^{c}\boldsymbol{Q} + p_{1_{pl}} = 0, \tag{97}$$

$$\delta \alpha_{z1}: \quad \nabla_2 \cdot \left(-\frac{h}{6}{}^{c}\boldsymbol{Q} + \nabla_2 \cdot \tilde{\boldsymbol{m}}\right) - \frac{2}{h}{}^{c}\overset{\langle 1 \rangle}{t} = 0 \tag{98}$$

and the boundary conditions

$$\delta w: \quad p^b_z = \boldsymbol{e}_\perp \cdot \left(\frac{d}{h}{}^{c}\boldsymbol{Q} + \nabla_2 \cdot \bar{\boldsymbol{m}}_S\right) + \frac{\partial}{\partial s}\bar{m}_{S_{\perp b}}, \tag{99}$$

$$\frac{\partial \delta w}{\partial s_\perp}: \quad \bar{m}^b_S = -\bar{m}_{S_{\perp\perp}}, \tag{100}$$

$$\delta \boldsymbol{\beta}_{pl}: \quad \boldsymbol{m}^b_{pl} = \boldsymbol{e}_\perp \cdot \overline{\boldsymbol{M}}, \tag{101}$$

$$\delta \alpha_{z1}: \quad {}^{c}q^b_{z1} = \boldsymbol{e}_\perp \cdot \left(-\frac{h}{6}{}^{c}\boldsymbol{Q} + \nabla_2 \cdot \tilde{\boldsymbol{m}}\right) - \frac{\partial}{\partial s}\tilde{m}_{\perp b}, \tag{102}$$

$$\frac{\partial \delta \alpha_{z1}}{\partial s_\perp}: \quad -\tilde{m}^b_{\perp\perp} = -\tilde{m}_{\perp\perp}. \tag{103}$$

The equilibrium conditions (88), (96), (97) and the boundary conditions (91), (99), (101) describe the five DOF theory by Reissner/Mindlin, which corresponds to the classic SWMT, if the skin bending and the longitudinal core stiffness are neglected (see (61): $\bar{\boldsymbol{m}}_S \Rightarrow 0$ and (60) ${}^{c}\boldsymbol{n} \Rightarrow 0$). These equations basically describe the global structural behaviour of SW-structures. Local effects are described by the remaining equations, which result from the extended kinematics, taking into account the core deformation and the independent skin bending. Removing the 8th DOF α_{z2} and neglecting the terms for the core warping (${}^{c}\boldsymbol{n} \Rightarrow 0$, ${}^{c}\boldsymbol{m} \Rightarrow 0$, $\tilde{\boldsymbol{n}} \Rightarrow 0$, $\tilde{\boldsymbol{m}} \Rightarrow 0$), the 7-DOF-theory (Kühhorn, 1991, 1993; Kühhorn and Schoop, 1992), results.

3. Numerical evaluation of instability cases

The assessment of the quality of the presented SW-theory is realised using reference solutions for the plate strip (assuming a width of $b = 1$ and a plane strain state), which are computed using the Finite Element Method (FEM). For this purpose a periodic solution without any disturbances is generated using a skilful load application. The use of plane eight-node continuum elements with reduced integration and a sufficient mesh density guarantees that the FEM-solution can be classified as an "exact" solution. These reference solutions are compared with the solutions resulting from the specialisation of the nonlinear equations (Section 2.5.2) with respect to the second-order theory.

Exemplarily, the results for symmetric skin wrinkling and for wrinkling of one skin are presented, while the antimetric skin wrinkling is left out (for further details see Golze (2000)).

The computation is exemplarily carried out using isotropic core and skin material with a common stiffness relation from Wiedemann (1986):

$$ {}^{s}E/{}^{c}E = 480 \quad \text{and} \quad {}^{s}\nu = 0.3 \text{ as well as } {}^{c}\nu \equiv 0 \tag{104} $$

Two characteristic cases are considered for evaluation purposes, namely

$$ \mathbf{I}: \quad \text{“thick” skins (longer-waved)with} \quad \frac{d = h + t}{t} = 10 \tag{105} $$

$$ \mathbf{II}: \quad \text{“thin” skins (short-waved)with} \quad \frac{d = h + t}{t} = 40, \tag{106} $$

where the short-wave case II (half wave length $\approx 0.4d$) is more difficult to describe but the relevant case in practice.

The solutions for the cases **I** and **II** will be compared applying:

A: *Extended SW-theory with eight DOF* and consideration of core warping. This theory corresponds to the one presented in this paper.
B: *Extended SW-theory with seven DOF* neglecting core warping according to Kühhorn (1991, 1993) and Kühhorn and Schoop (1992).
C: *FEM-solution* (plain strain) as described above.

The relevant wrinkling stress (critical stress) σ_{xx_K} in the compressively loaded SW-skin is related to ${}^{s}E$ and plotted over the normalized half wave length a/d (Figs. 14–17). Additionally, in the Figs. 14–17 the eigenvectors at curve minimum according to theory A are presented. The solution of the instability cases (Golze (2000)) is realised using appropriate wave approaches such as $\Xi = \hat{\Xi}\cos(\frac{\pi}{a}x)$ whereby Ξ represents a DOF according to (30).

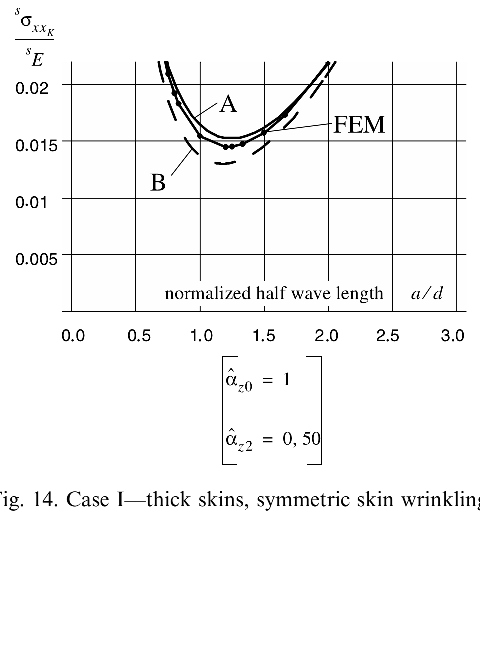

Fig. 14. Case I—thick skins, symmetric skin wrinkling.

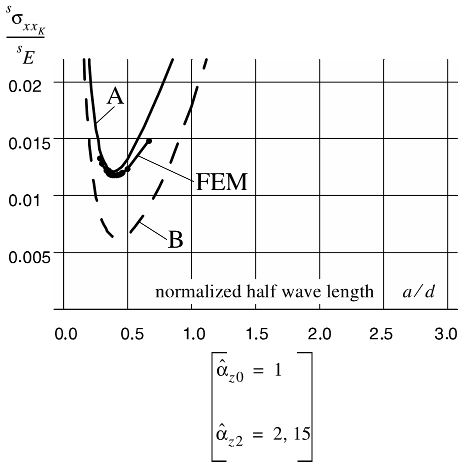

Fig. 15. Case II—thin skins, symmetric skin wrinkling.

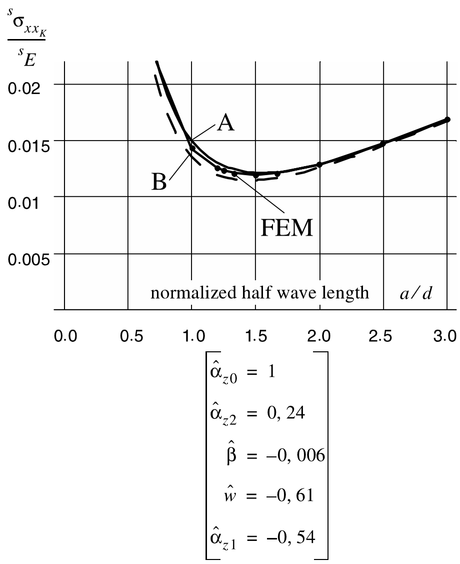

Fig. 16. Case I—thick skins, one side wrinkling.

3.1. Symmetric skin wrinkling

Associated evaluations are shown in Figs. 14 and 15. Fig. 14 shows a good match for case I in which thick skins are considered, where results from theory A, presented in this paper, are located even closer to the reference solution. The eigenvector illustrates the dominance ($\hat{\alpha}_{z0} > \hat{\alpha}_{z2}$) of the bellied, quadratic part of core warping (see Fig. 9B). The wrinkling half wave length a is computed to about 1.2-fold of the skin midsurface distance $d = h + t$ whereby the appearance of longer waves in this case I is documented.

In case II of thin skins (Fig. 15) a considerable improvement results from theory A, so that the solution for this short-wave case of $a/d \approx 0.4$ is mostly corresponding to the reference solution. This time the

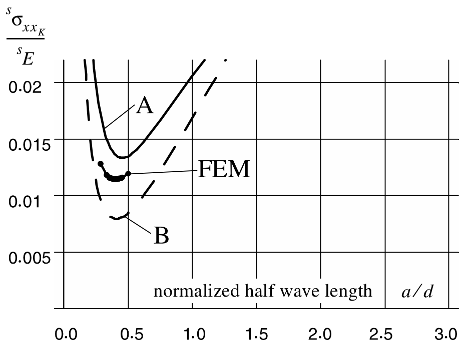

$$\begin{bmatrix} \hat{\alpha}_{z0} = 1 \\ \hat{\alpha}_{z2} = 2,08 \\ \hat{\beta} = 0,007 \\ \hat{w} = -0,46 \\ \hat{\alpha}_{z1} = -1,41 \end{bmatrix}$$

Fig. 17. Case II—thin skins, one side wrinkling.

eigenvector ($\hat{\alpha}_{z2} > \hat{\alpha}_{z0}$) shows a strong dominance of the warping contribution with 4th power in z-direction (see Fig. 9D) and the corresponding contributions from linear core shear- and quadratic thickness strain.

3.2. Single-side skin warping

Again Fig. 16 shows a good match for case I (thick skins) with a closer approximation of A. The minimum failure load appears at half wave lengths of about 1.5-fold d. For case II (thin skins, Fig. 17) A results in a stiffer and B in a weaker solution with regard to the reference solution. A shows the closer correlation. The eigenvector shows the dominance of $\hat{\alpha}_{z1}$ and $\hat{\alpha}_{z2}$ (Fig. 9C and D) and thus the significance of these DOF.

4. Summary

The geometrically nonlinear theory for plane SW-structures using eight kinematic degrees of freedom $(\boldsymbol{r}, \boldsymbol{d}, \alpha_{z1}, \alpha_{z2})$ described in this paper is applicable for arbitrary displacements and rotations with the restriction to moderate strains. From the detailed consideration of the core deformation with respect to cross-section warping as well as transversal and shear stiffness and with consideration of independent skin bending, an extensive and closed description of the global and local (load application, skin wrinkling,...) SW-structural behaviour becomes possible. The nonlinear equations (Section 2.5.2) include simple specialization with respect to the first or second-order theory. The effectiveness of the theory with respect to the prediction of skin wrinkling is demonstated applying a plate strip subjected to a compressive (symmetric mode) and bending moment load (wrinkling of only one skin) as example. Corresponding numerical investigations prove the efficiency of the theory if the wrinkling half wavelength is greater than 0.4 times the core thickness, a condition which holds for a lot of applications (Wiedemann, 1986). For shorter wavelengths the assumption of quadratic thickness strain distribution becomes too crude and therefore the applicability is limited.

References

Bischoff, M., Ramm, E., 2000. On the physical significance of higher order kinematic and static variables in a three-dimensional shell formulation. Int. J. Solids Struct. 37, 6933–6960.

Büchter, N., Ramm, E., Roehl, D., 1994. Three-dimensional extension of nonlinear shell formulation based on the enhanced assumed strain concept. Int. J. Num. Methods Eng. 37, 2551–2568.

Frostig, Y., 1998. Buckling of sandwich panels with a flexible core-high order theory. Int. J. Solids Struct. 35, 183–204.

Golze, M., 2000. Untersuchungen zum Knitterverhalten (lokale Instabilitäten) ebener Sandwichtragwerke unter Heranziehung einer verfeinerten Theorie mit quadratischer Dickenverzerrung. Diplomarbeit Technische Universität Berlin, BTU Cottbus.

Krätzig, W.B., 1993. 'Best' transverse shearing and stretching shell theory for non-linear finite element simulations. Comput. Methods Appl. Mech. Eng. 103, 135–160.

Kühhorn, A., 1993. Nichtlineare Theorie und finites Element für Sandwichtragwerke zur Beschreibung des globalen und lokalen (Knittern) Versagens. ZAMM Z. Angew. Math. Mech. 73 (4–5), T438–T443.

Kühhorn, A., 1991. Geometrisch nichtlineare Theorie für Sandwichschalen unter Einbeziehung des Knitterphänomens. VDI-Verlag, Reihe 18, no. 100.

Kühhorn, A., Schoop, H., 1992. A nonlinear theory for sandwich shells including the wrinkling phenomenon. Arch. Appl. Mech. 62, 413–427.

Kühhorn, A., Silber, G., 2000. Technische Mechanik für Ingenieure. Hüthig, Heidelberg.

Mindlin, R., 1951. Influence of rotatory inertia and shear on flexural vibrations of isotropic, elastic plates. J. Appl. Mech. 18, 31–38.

Naghdi, P.M., 1972. The theory of shells. In: Flügge, S. (Ed.), Handbuch der Physik, vol. VI/2, Springer, Berlin.

Plantema, F.J., 1966. Sandwich Construction. John Wiley and Sons, New York.

Reissner, E., 1945. The effect of transverse shear deformation on the bending of plates. J. Appl. Mech. 12, 69–77.

Schoop, H., 1999. Finite–Elemente-Methode für Platten und Scheiben. Skriptum zur gleichnamigen Vorlesung. Technische Universität Berlin.

Schoop, H., 1988. Schnittlasten dickenelastischer Schalen. In: Mechanikbeiträge zu Theorie und Anwendungen zum 60. Geburtstag von Prof. Dr. Trostel. Technische Universität Berlin.

Simo, J.C., Rifai, S., Fox, D., 1990. On a stress resultant geometrically exact shell model. Part IV: Variable thickness shells with through-the-thickness stretching. Comput. Methods Appl. Mech. Eng. 81, 91–126.

Stamm, K., Witte, H., 1974. Sandwichkonstruktionen–Berechnung, Fertigung, Ausführung. Springer, Wien.

Trostel, R., 1988. Gedanken zur Konstruktion mechanischer Theorien II. In: Forschungsber. No. 7. Technische Universität Berlin, Inst. für Mechanik.

Trostel, R., 1985. Gedanken zur Konstruktion mechanischer Theorien. In: Trostel, R. (Ed.), Beiträge zu den Ingenieurwissenschaften. Universitätsbibliothek TU Berlin, pp. 96–134.

Vonach, W.K., Rammerstorfer, F.G., 2001. A general approach to the wrinkling instability of sandwich plates. Struct. Eng. Mech. 12, 336–376.

Vonach, W.K., Rammerstorfer, F.G., 2000. Wrinkling of thick orthotropic sandwich plates under general loading conditions. Arch. Appl. Mech. 70, 338–348.

Wiedemann, J., 1986. Leichtbau: Band 1—Elemente. Springer, Berlin.